Vietnam Journal of Chemistry, International Edition, **54**(6): 704-709, 2016
DOI: 10.15625/0866-7144.2016-00391

High-energy ball milling preparation of $La_{0.7}Sr_{0.3}MnO_3$ and $(Co,Ni)Fe_2O_4$ nanoparticles for microwave absorption applications

Chu Thi Anh Xuan[1,2], Ta Ngoc Bach[1], Tran Dang Thanh[1], Ngo Thi Hong Le[1], Do Hung Manh[1], Nguyen Xuan Phuc[1], Dao Nguyen Hoai Nam[1*]

[1]*Institute of Materials Science, Vietnam Academy of Science and Technology*

[2]*Department of Physics, University of Science, Thai Nguyen University*

Received 5 August 2016; Accepted for publication 19 December 2016

Abstract

Microwave and radar absorbing materials (MAM and RAM) are widely used for reducing electromagnetic interference (EMI) for electronic equipment and devices, in electromagnetic anechoic technique, and especially in radar stealth technology. Ferromagnetic and ferrimagnetic nanoparticles have been known to have a strong microwave absorbing capability. To study magnetic MAMs and RAMs, we have prepared $La_{0.7}Sr_{0.3}MnO_3$ ferromagnetic and several $(Co,Ni)Fe_2O_4$ ferrimagnetic nanoparticle powders using high-energy ball milling technique, which is capable of producing nanoparticles in reasonably larger scale comparing to conventional chemical methods. The magnetic properties of the nanoparticle powders are strongly dependent on the preparation conditions. The milling process produces damages and defects not only on the surface, but also the crystal structure inside the particles, that cause an undesired strong reduction of saturation magnetization (M_s) and an increase of coercivity (H_c). A suitable post-milling heat treatment is able to heal the particles and recover most of their saturation magnetization and magnetic softness. The nanoparticles are then mixed with paraffin for microwave and radar absorption measurements.

Keywords. Microwave absorbing materials, radar absorbing materials, electromagnetic interference, stealth technology, magnetic nanoparticles.

1. INTRODUCTION

As electronic and radio devices are more and more densely packed in mobile vehicles like submarines, ships, airplanes, satellites, etc. electromagnetic interference (EMI) becomes an emerging problem [1]. Faraday cage has been well known as the most effective method for shielding its interior from electromagnetic radiation. However, since the cage cannot be properly grounded in mobile vehicles, it may generate secondary radiation that affects nearby unshielded instruments. Instead of reflecting electromagnetic radiation away from objects that need to be shielded, one can also use specially designed materials that absorb electromagnetic wave and converts its energy into heat. This technique is essential in stealth technology where reflection of the incident radiation is absolutely unwanted.

Recent studies have found that ferromagnetic nanoparticles are the most effective microwave absorbers (MAM). The best performance MAM was found for the mixture of carbonyl Fe and $BaTiO_3$ in epoxy, which gives a reflection loss (*RL*, defined below) as low as -64 dB [2]. The absorbing mechanism in magnetic nanoparticles is still not very clear as whether it comes from the ferromagnetic resonance or the relaxation loss; both of them depend on magnetic anisotropy (K_a) and relative permeability (μ_r). Higher μ_r, therefore lower coercivity H_c and higher saturation magnetization M_s, is always required for a MAM to have stronger microwave absorption. Since the practical performance of a MAM is characterized by its capability of both absorption and reflection of microwave, one uses the reflection loss defined as $RL(dB) = 10log\frac{P_i}{P_r}$ (where P_i and P_r are the powers of the incident and reflected waves, respectively). Experimental *RL* value can be calculated using the NSW algorism proposed by Nicolson and Ross [3] and Weir [4] based on the transmission line theory [5]:

$$Z = \sqrt{\mu_r/\varepsilon_r}\tanh[-i(2\pi d/\lambda)\sqrt{\varepsilon_r\mu_r}] \quad (1)$$

$$RL\ (dB) = 20\log|(Z - Z_0)/(Z + Z_0)| \quad (2)$$

Here, Z is the sample's impedance, Z_0 is the impedance of the air (which is supposed to be ~377 Ω as of vacuum), ε_r and μ_r are the relative permittivity and permeability, respectively, d is the thickness of the MAM layer, and λ is the wavelength of the incident wave. *RL* is considered the most important parameter that characterizes the absorption capability of microwave absorbers.

For practical use, magnetic oxides are preferred fillers in MAMs since they are durable and have good corrosion resistance. Among them, magnetic ferrites such as $(Co,Ni)Fe_2O_4$ have been widely studied for microwave absorption applications [6, 7]. Ferrite nanoparticles are usually prepared by chemical reaction methods such as sol-gel, co-precipitation, and thermal hydrolysis, etc. While the microwave measurements as well as the applications of MAMs always require a large amount of materials, large scale preparation of oxide nanoparticles using these chemical methods in laboratory condition is not very practical. Here we report a top-down method for the preparation of $La_{0.7}Sr_{0.3}MnO_3$ and $(Co,Ni)Fe_2O_4$ nanoparticles by combining the conventional solid state reaction synthesis usually used for ceramics with a high-energy ball milling technique and proper post-milling thermal annealing processes. Our results show the feasibility of producing large amount of high quality nanoparticles which can be used for microwave shielding studies and applications.

2. EXPERIMENTAL

2.1. Sample preparation

Polycrystalline bulk samples were prepared using the conventional solid state reaction method. Appropriate amounts of raw materials were thoroughly mixed and ground, pressed into pellets, and sintered at 1100 ^oC for 5 h in air. The grinding and sintering processes were repeated several times to ensure the material's crystallization and homogeneity. The obtained bulk compounds were milled into nanoparticles by a high energy ball miller for 0.5 h. The nanoparticle powders were then annealed at different temperatures for healing damages caused by the milling process. Absorption layers of $La_{0.7}Sr_{0.3}MnO_3$ and $(Co,Ni)Fe_2O_4$ are prepared by coating the mixture of the nanoparticles and paraffin on a mica substrate.

2.2. Measurement techniques

The quality of the sample was frequently checked at every step during preparation via X-ray diffraction (XRD, SIEMENS D5000) and room temperature magnetization (VSM, noncommercial system) techniques. The XRD is also used to determine the average size of the nanoparticles using the Scherrer's formula [8], $D = \frac{K\lambda}{\beta cos\theta}$, where K is the shape factor taken as 0.9, λ is the X-ray wavelength, β is the line broadening at half the maximum intensity (FWHM) in radians, and θ is the Bragg angle. Scanning Electron Microscopy (SEM, Hitachi S-4800) images were also taken to examine the size distribution of the nanoparticles.

Free-space microwave transmission and reflection measurements were performed by a vector network analyzer (VNA). In the transmission measurements, the areas surrounding the sample were covered by metal shields so that the receiver only received electromagnetic wave that went through the sample. In the reflection measurements, the metal shields were removed so that only the wave reflected from the samples surface can reach the receiver. The angle between the incident radiation and the sample's plane is 45^o in both cases.

3. RESULTS AND DISCUSSION

3.1. $CoFe_2O_4$ ferrite

Figure 1a presents the XRD patterns for the bulk and nanoparticle powder of the $CoFe_2O_4$ ferrite. The bulk sample is single phase with no trace of any secondary phases or impurities; all the peaks could be indexed to the standard spinel structure of $CoFe_2O_4$ [9]. For the as-milled powder, the pattern is much noisier with a raised background and broadened peaks; however, no extra peak can be observed. After annealed at 900 ^oC for 2 h, the powder exhibits a pattern that is very similar to that of the bulk sample. Applying the Scherrer's equation to the broadening of the XRD peaks, we obtained the mean size of the grains or particles D = 47.0, 29.3 and 46.0 nm for the bulk, as-milled, and 900 ^oC annealed samples, respectively.

The magnetic hysteresis loops of $CoFe_2O_4$ at room temperature are plotted in figure 1b. The bulk sample shows M_s~77 emu/g (at 10 kOe) and H_c~1 kOe, which are comparable with previous values reported by other authors [10, 11]. After the high energy milling, M_s is reduced to ~56 emu/g while a huge H_c increase is observed. Annealing the nanoparticle powder at 900 ^oC for 2 h recovers almost fully the M_s, and significantly reduces the H_c.

All the characteristic parameters of the $CoFe_2O_4$

samples are summarized in table 1a.

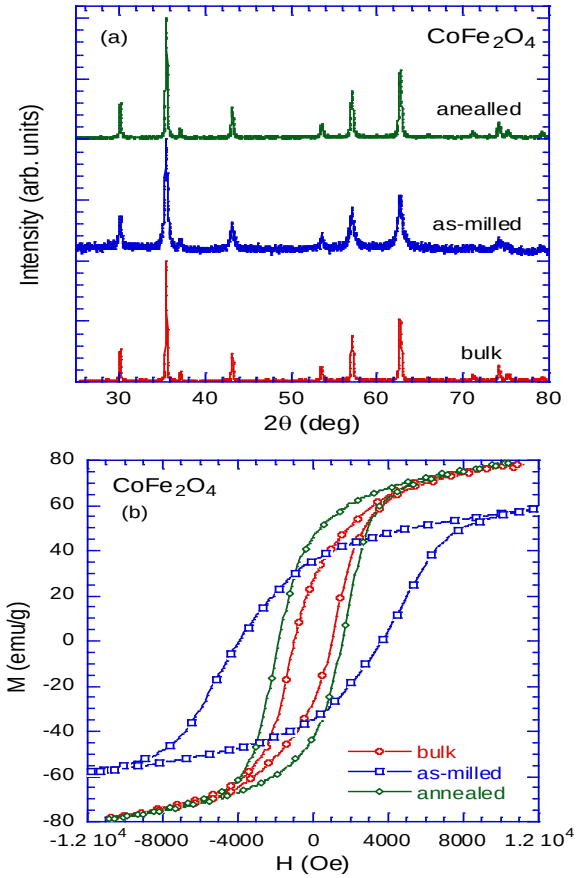

Figure 1: XRD spectra (a) and *M*(*H*) loops (b) of the $CoFe_2O_4$ bulk, as-milled nanopowder, and 900 ^oC annealed nanopowder samples measured at room temperature

3.2. $NiFe_2O_4$ ferrite

Typical XRD spectra of the $NiFe_2O_4$ are illustrated in figure 2a. All the samples are single phase with the expected spinel structure [12, 13]. Similar to the case of the $CoFe_2O_4$ samples, after the sample is milled into nanoparticles, the XRD spectrum becomes noisier with a raised background signal and broadened peaks. No extra peak would be observed after the milling. Annealing the milled powder helps bring the spectra back to near that of the bulk sample. From the XRD data, the mean sizes of the nanoparticles, as listed in table 1, are calculated using the Scherrer's formula.

As shown in figure 2b for the *M*(*H*) hysteresis loops, $NiFe_2O_4$ has quite a good magnetic softness. The M_s and H_c values are comparable to those previously reported [14, 15]. Although the M_s (~44.6 emu/g for the bulk sample at 10 kOe) is considerably smaller than that of $CoFe_2O_4$, the coercivities of the bulk sample and the 900 ^oC annealed nanopowder are very small (H_c~72Oe). The milling process increases H_c to ~967 Oe while reducing M_s to about 34.5 emu/g. After annealing at 900 ^oC for 2h, M_s is partially recovered and raised back to ~41.3 emu/g. Table 1b summarizes the characteristic parameters of the $NiFe_2O_4$ samples.

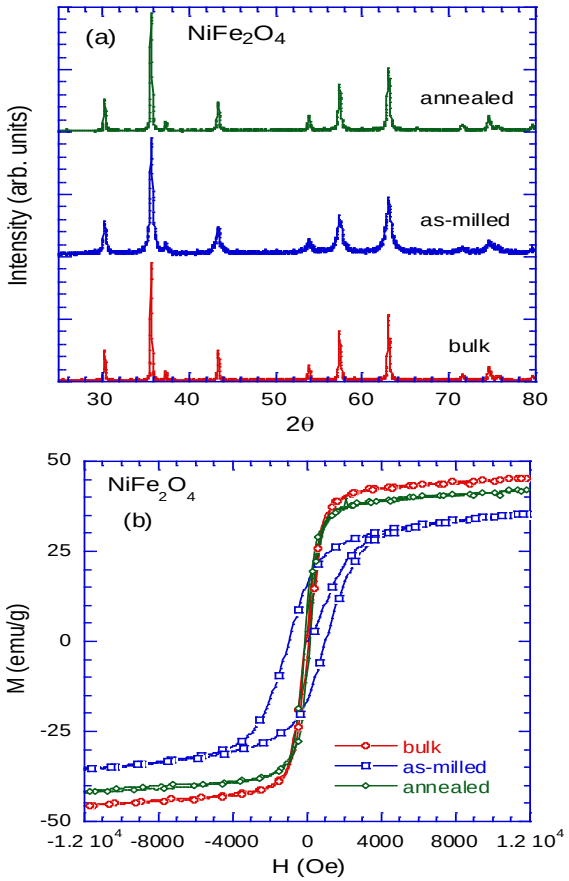

Figure 2: XRD spectra (a) and *M*(*H*) loops (b) of the $NiFe_2O_4$ bulk, as-milled nanopowder, and 900 ^oC annealed nanopowder samples measured at room temperature

3.3. $La_{0.7}Sr_{0.3}MnO_3$ ferromagnet

The bulk sample shows a clean XRD pattern indicating a single phase of $La_{0.7}Sr_{0.3}MnO_3$ similar to that previously reported [16]. Qualitatively, the high energy milling process influences the structural and magnetic properties of the $La_{0.7}Sr_{0.3}MnO_3$ sample in a similar manner with the ferrites. The XRD patterns in figure 3a show a broadening of the diffraction peaks caused by the milling, indicating a reduction of the particle size to the order of the grain size in the bulk. However, the milling influence is not as strong as in the case with the ferrites: the peaks are only slightly broadened and the background noise seems unchanged. The milling also does not produce any impurity or secondary phases.

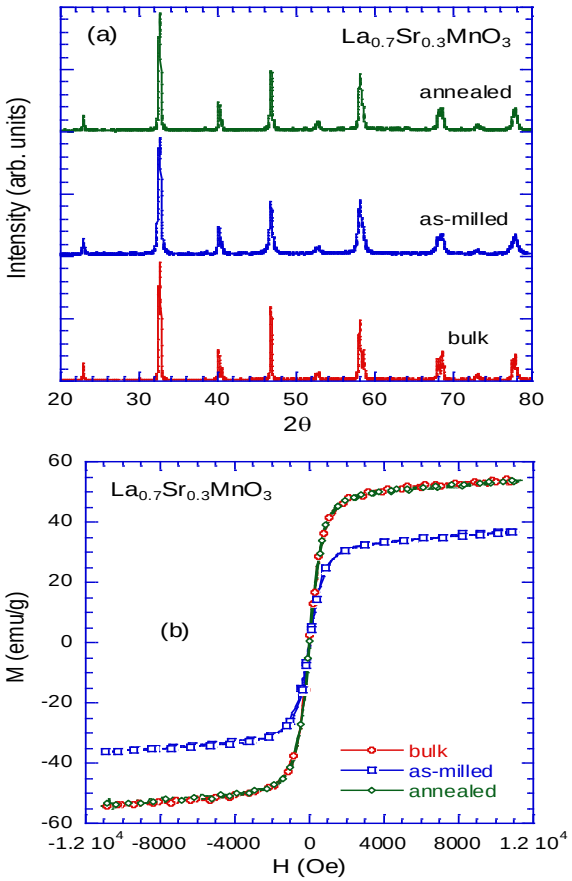

Figure 3: Room temperature XRD spectra (a) and $M(H)$ loops (b) of the $La_{0.7}Sr_{0.3}MnO_3$ bulk, as-milled nanopowder, and 900 ^oC annealed nanopowder samples

The $M(H)$ measurements in figure 3b indicate that $La_{0.7}Sr_{0.3}MnO_3$ is a very soft ferromagnet. The H_c of the bulk sample is almost undetectable using our noncommercial VSM system while that of the as-milled sample is just about 20 Oe. The bulk sample has M_s of ~53 emu/g (almost the same as reported in [17]) and is also significantly reduced by the milling process. Interestingly, the $M(H)$ loops of the 900 ^oC annealed sample and the bulk sample are almost identical.

The characteristic parameters of the $La_{0.7}Sr_{0.3}MnO_3$ samples are listed in table 1c.

In macroscopic samples, where contribution from the surfaces is small, the magnetic property is governed by the bulk. With decreasing the sample's dimensions, the magnetic contribution from the surface becomes significant and is even very profound in nanoparticles. That explains the strong increase in H_c of the as-milled samples comparing to the bulk ones due to the dominant role of surface magnetic anisotropy [18]. The surface imperfections such as broken bonds, lattice defects and vacancies, etc. also cause a reduction of the saturation magnetization. Surface disorder can therefore form a "shell" covering the nanoparticle that contributes only very little to M_s but creates large surface random anisotropies, causing a considerable enhancement of H_c. Reduction of M_s and enhancement of H_c are both detrimental to the microwave absorption capability of MAMs. Unfortunately, these effects are even stronger in the case of high energy milling; the milling not only causes severe surface damages, but also defections on the crystal lattice inside the core of the nanoparticles. This could be considered the most disadvantage feature of the higher energy milling compared to the chemical methods for the fabrication of nanoparticles.

Table 1: Room temperature characteristic parameters of the studied samples (D are derived from the XRD data using Scherrer's formula, M_s is determined at 10 kOe)

	D (nm)	M_s (emu/g)	H_c (Oe)
a. $CoFe_2O_4$			
Bulk	47.0	77.0	1000
As-milled	29.3	56.0	3791
Annealed (900 ^oC, 2h)	46.0	78.0	1667
b. $NiFe_2O_4$			
Bulk	44.9	44.6	72
As-milled	18.8	34.5	967
Annealed (900 ^oC, 2h)	38.7	41.3	128
c. $La_{0.7}Sr_{0.3}MnO_3$			
Bulk	54.5	53.0	5
As-milled	32.3	36.3	23
Annealed (900 ^oC, 2h)	38.6	54.0	13

In order to heal the damages caused by the milling, post-milling heat treatments may be employed. We annealed the nanopowder at different temperatures (for clarity, we present only the results for three typical samples: bulk, as-milled, and annealed at 900 ^oC) and observed that the particle size was increased by annealing; a higher annealing temperature leaded to greater size of the particles. The annealing might (i) reduce the lattice defects inside the particle core, (ii) recrystallize the disordered shell, and (iii) coalesce the particles to

bigger ones. The results in tables 1a and 1b clearly show a strong increase in the mean particle size by annealing $CoFe_2O_4$ and $NiFe_2O_4$ at 900 ^oC for 2 h. Such a large gain of *D* would indicate that there were coalescences of the small particles into bigger ones. To reduce the coalescence of particles, lower annealing temperature and/or shorter annealing time should be applied. In the case of $La_{0.7}Sr_{0.3}MnO_3$, *D* just only slightly increases from 32.3 to 38.6 nm, evidencing perhaps only the recrystallization of the particle shell. Along with the increase in *D*, a reduction of H_c and a recovery of M_s are also observed. It is interesting that the nanoparticles of $La_{0.7}Sr_{0.3}MnO_3$ could fully recover their M_s by the annealing without increasing much of the particle size. With a reasonable M_s and a very small H_c, $La_{0.7}Sr_{0.3}MnO_3$ is expected to be a good filler for MAMs.

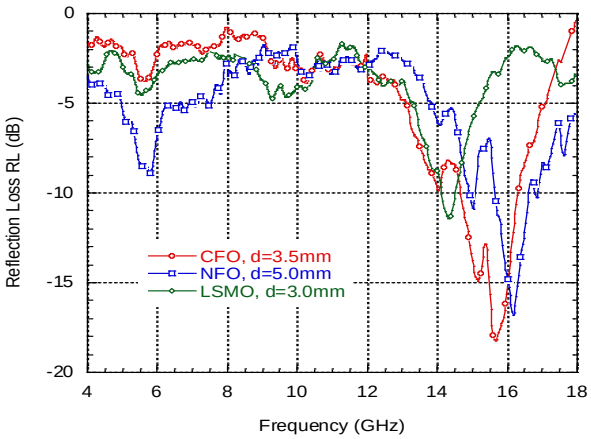

Figure 4: Reflection Loss, *RL*, of the $CoFe_2O_4$ (red, circle symbols), $NiFe_2O_4$ (blue, squares), and $La_{0.7}Sr_{0.3}MnO_3$ (green, diamonds) nanopowders mixed in paraffin. The mixtures are casted to flat plates with different thicknesses of 3.5, 5.0, and 3.0 mm for $CoFe_2O_4$, $NiFe_2O_4$, and $La_{0.7}Sr_{0.3}MnO_3$, respectively

To demonstrate the microwave absorption capability, the obtained nanopowders are then mixed with paraffin and casted into flat plates with different thicknesses for microwave measurements. We present in figure 4 the typical data of *RL* within the radar range of frequency (4-18 GHz) for $CoFe_2O_4$, $NiFe_2O_4$, and $La_{0.7}Sr_{0.3}MnO_3$ plates with thicknesses of 3.5, 5.0, and 3.0 mm, respectively. All three samples show clear drops in *RL* in the high frequency range above 14 GHz, indicating considerable radar absorbability of the materials. The absorbability can be further improved by optimizing the plate's thickness, the nanopowder fraction, as well as the nanoparticle grain sizes. Stronger absorption will give larger negative value of *RL*.

4. CONCLUSION

We have demonstrated a method of using a high energy mill in combination with conventional solid state reaction synthesis and post-milling heat treatments for fabricating oxide nanoparticles. High quality nanoparticles could be obtained by employing appropriate post-milling heat treatments. This method can produce a large amount of nanoparticles in the laboratory condition; it is therefore suitable for fabricating nanoparticle fillers for MAMs. The obtained $CoFe_2O_4$, $NiFe_2O_4$ and $La_{0.7}Sr_{0.3}MnO_3$ nanopowders have excellent phase quality and magnetic properties required for high performance MAMs. The MAM plates of the obtained nanopowders mixed in paraffin show considerable absorbability in the radar frequency range.

Acknowledgment. T*his work was sponsored by the Vietnam National Foundation for Science and Technology Development (NAFOSTED) under Grant number 103.02-2012.58.*

REFERENCES

1. D. D. L. Chung. *Electromagnetic interference shielding effectiveness of carbon materials*, Carbon, **39**, 279 (2001).
2. Q. Yuchang, Z. Wancheng, L. Fa, and Z. Dongmei. *Optimization of electromagnetic matching of carbonyl iron/$BaTiO_3$ composites for microwave absorption*, J. Mag. Magn. Mater., **323**, 600 (2011).
3. A. M. Nicolson and G. F. Ross. *Measurement of the Intrinsic Properties of Materials by Time-Domain Techniques*, IEEE Trans. Instrum. Meas., **IM-19**, 377 (1970).
4. W. B. Weir. *Automatic measurement of complex dielectric constant and permeability at microwave frequencies*, Proc. IEEE, **62**, 33 (1974).
5. Y. Naito and K. Suetake. *Application of Ferrite to Electromagnetic Wave Absorber and Its Characteristics*, Theory Tech. MITT, **19**, 65 (1971).
6. J. Cao, W. Fu, H. Yang, Q. Yu, Y. Zhang, S. Liu, P. Sun, X. Zhou, Y. Leng, S. Wang, B. Liu, and G. Zou. *Large-Scale Synthesis and Microwave Absorption Enhancement of Actinomorphic Tubular ZnO/$CoFe_2O_4$ Nanocomposites*, J. Phys. Chem. B, **113** 4642 (2009).
7. X. Gu, W. Zhu, C. Jia, R. Zhao, W. Schmidt, and Y. Wang, *Synthesis and microwave absorbing properties of highly ordered mesoporous crystalline $NiFe_2O_4$*, Chem. Commun., **47**, 5337 (2011).
8. A. L. Patterson. *The Scherrer Formula for X-Ray*

Particle Size Determination, Phys. Rev., **56**, 978 (1939).
9. W. H. Wang, and X. Ren, *Flux growth of high-quality $CoFe_2O_4$ single crystals and their characterization*, J. Crys. Growth, **289**, 605 (2006).
10. Y. X. Zheng, Q. Q. Cao, C. L. Zhang, H. C. Xuan, L. Y. Wang, D. H. Wang, and Y. W. Du. *Study of uniaxial magnetism and enhanced magnetostriction in magnetic-annealed polycrystalline $CoFe_2O_4$*, J. Appl. Phys., **110**, 043908 (2011).
11. A. Muhammad, R. Sato-Turtelli, M. Kriegisch, R. Grössinger, F. Kubel, and T. Konegger. *Large enhancement of magneto striction due to compaction hydrostatic pressure and magnetic annealing in $CoFe_2O_4$*, J. Appl. Phys., **111**, 013918 (2012).
12. P. Sivakumar, R. Ramesh, A. Ramanand, S. Ponnusamy, and C. Muthamizhchelvan. *Synthesis, studies and growth mechanism of ferromagnetic $NiFe_2O_4$ nanosheet*, Appl. Surf. Sci., **258**, 6648 (2012).
13. H. Zhao, X. Sun, C. Mao, and J. Du. *Preparation and microwave–absorbing properties of $NiFe_2O_4$-polystyrene composites*, Physica B, **404**, 69 (2009).
14. F. L. Zabotto, A. J. Gualdi, and J. A. Eiras. *Influence of the Sintering Temperature on the Magnetic and Electric Properties of $NiFe_2O_4$ Ferrites*, Mat. Res., **15**, 428 (2012).
15. L. Lv, J-P. Zhou, Q. Liu, G. Zhu, X-Z. Chen, X-B. Bian, and P. Liu. *Grain size effecton the dielectric and magnetic properties of $NiFe_2O_4$ ceramics*, Physica E, **43**, 1798 (2011).
16. D. N. H. Nam, L. V. Bau, N. V. Khiem, N. V. Dai, L. V. Hong, N. X. Phuc, R. S. Newrock, and P. Nordblad. *Selective dilution and magnetic properties* of $La_{0.7}Sr_{0.3}Mn_{1-x}M_xO_3$ (M = Al, Ti), Phys. Rev. B, **73**, 184430 (2006).
17. A. Gaur, and G. D. Varma. *Magnetoresistance behaviour of $La_{0.7}Sr_{0.3}MnO_3/NiO$ composites*, Solid State Commun., **139**, 310 (2006).
18. D. A. Garanin and H. Kachkachi. *Surface Contribution to the Anisotropy of Magnetic Nanoparticles*, Phys. Rev. Lett., **90**, 065504 (2003).

Corresponding author: **Dao Nguyen Hoai Nam**
Institute of Materials Science, Vietnam Academy of Science and Technology
18, Hoang Quoc Viet Road, Cau Giay District, Hanoi, Vietnam
E-mail: daonhnam@yahoo.com.